Earth Planets Space, **51**, 93–106, 1999

Holocene geomagnetic secular variations recorded by sediments from Escondido Lake (south Argentina)

C. S. G. Gogorza[1], A. M. Sinito[1,5], I. Di Tommaso[2], J. F. Vilas[2,5], K. M. Creer[3], and H. Nuñez[4]

[1]*IFAS-UNCPBA, Pinto 399, 7000 Tandil, Argentina*
[2]*Laboratorio Daniel Valencio-UBA - Ciudad Universitaria, Pab 2, 1428, Buenos Aires, Argentina*
[3]*Department of Geology and Geophysics, University of Edinburgh, West Main Road, Edinburgh EH9 3JW, U.K.*
[4]*Instituto Antartico Argentino, Cerrito 1248, Buenos Aires, Argentina*
[5]*CONICET, Rivadavia 1917, 1033, Buenos Aires, Argentina*

(Received January 26, 1998; Revised October 16, 1998; Accepted October 21, 1998)

Paleomagnetic and sedimentological studies carried out on two short cores and nine long cores from the bottom sediments from Escondido Lake (south-western Argentina) are described.

Rock magnetic analysis suggests that the main carriers of magnetization seems to be ferrimagnetic minerals, predominantly pseudo single domain magnetite. The presence of greigite, as diagenetic *euxinic* material, is also suggested.

Calibrated ages were calculated from radiocarbon dating and a transfer function *shortened depth*-age is built, which suggests the existence of a hiatus, supported by the suggestion of previous palynological studies about the possible evidence of the younger Dryas cooling event seen in the Antarctic ice cores.

The stacked inclination and declination curves and their standard deviations using arithmetical average after chronostratigraphic correlations are made.

Inclination data show two well defined periods: a long period (about 7700 years) and a short one (between 2660 and 2900 years). Declination data show two intermediate periods (about 3600 and 2900 years respectively) and a long, although less reliable, period (about 10000 years). The longer periods may be related to dipolar variations, while the shorter periods may be associated to non dipolar variations.

1. Introduction

Paleomagnetic studies of Late Pleistocene-Holocene lake sediments carried out up to the present time in Europe, North America and Australia have revealed the existence of long period secular variations (LPSV) of the ancient geomagnetic field, in the order of a few thousand of years, in both declination and inclination. Paleomagnetic records show that LPSV can be correlated between sediment sequences on a regional basis and help to constrain models of core dynamo processes. Moreover, logs of the natural remanent magnetization (NRM) intensity and magnetic susceptibility can be used for lithostratigraphic correlation of Late Pleistocene-Holocene sediments within a particular depositional basin. Therefore paleomagnetic, rock magnetic, sedimentological, radiometric and palynological data from lake sediments can usefully be combined to define the paleolimnological and paleoenvironmental history of a geographical area.

The experimental results from South America are scarce. Creer *et al.* (1983) carried out paleomagnetic and sedimentological studies on sediments from cores obtained from lakes in southwestern Argentina. Gogorza *et al.* (1998) presented the preliminary results of sediments from two lakes of southwestern Argentina, namely Escondido and Moreno. In this work, we present the stacked Paleosecular Variation (PSV) curves obtained from the sediments from Escondido Lake and the spectral analysis of these PSV curves. The different chronological meaning of the tephra layers and their behaviour as magnetic recorder were taken into account, to construct reliable curves of PSV.

2. Geology and Setting

Escondido Lake is on the east side of the Andean Patagónica Cordillera; it is located in the Llao Llao area, San Carlos de Bariloche (about 41°S, 71°30′W), at an altitude of 800 m (Figs. 1(a) and (b)). The regional geological features of the Andean Patagónica Cordillera have been described by González-Bonorino (1979) and González-Díaz and Nullo (1980). Several authors, particularly Feruglio (1941) and González-Bonorino (1973, 1979), studied the geology and stratigraphy of the southern zone of Nahuel Huapi Lake area. The geology of the area is represented mainly by the Nahuel Huapi Group of early Cenozoic age. It has been subdivided into the mainly igneous Ventana Formation of Eocene age and the mainly sedimentary Ñirihuau Formation of Eocene-Oligocene age.

Granites and tonalites, which have been identified as belonging to the lower Paleozoic, are also exposed (González-Bonorino, 1973).

The exposed holocene rocks consist principally of glacial and fluvio-glacial sediments and abundant volcanic ash layers, which grow thicker westwards, where the main effusive centers are located.

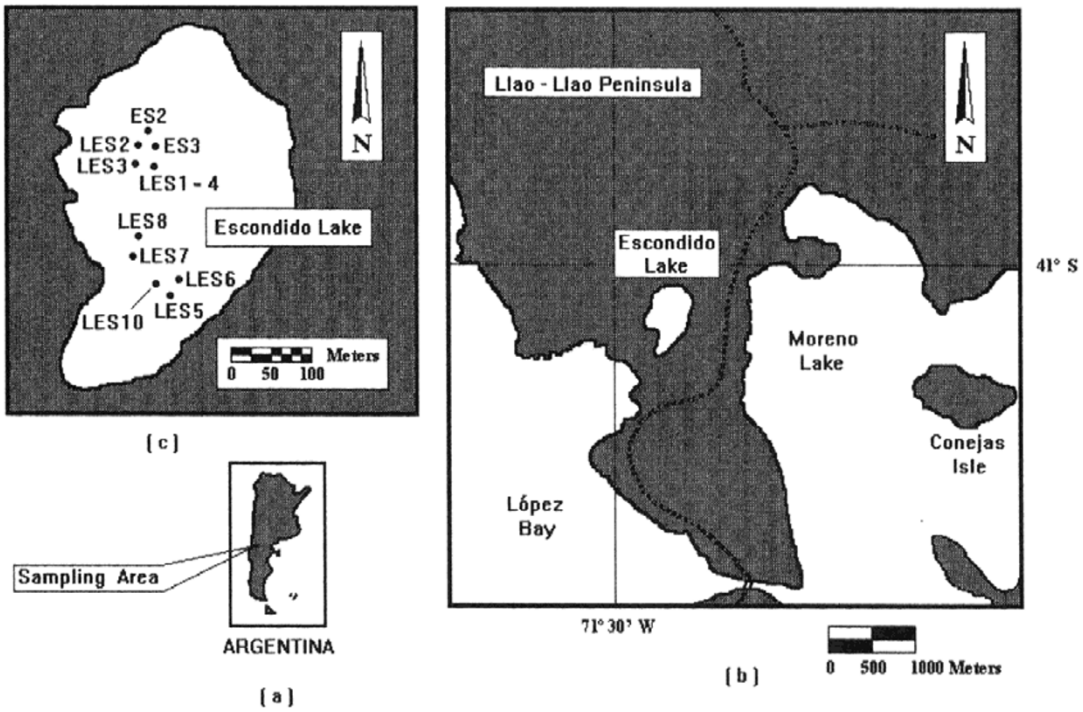

Fig. 1. (a) and (b) Geographical location of Escondido Lake; (c) location of coring sites in the lake.

Table 1. Data from core sampling.

Core name	Length (cm)	N_p	N_d
les1	263	114	0
les2	417.5	181	8
les3	335.5	146	0
les4	269	113	0
les5	398.5	145	0
les6	396	160	1
les7	358	151	0
les8	384	163	0
es2	43	45	0
es3	41	50	2

N_p: number of paleomagnetic samples.
N_d: number of dating samples.

3. Field Work and Sampling

In order to avoid the effects of turbidity currents and other sources of potential post-depositional disturbance of sediments, and to guarantee a low deposition rate, a small lake was deliberately chosen. Short cores—up to 1.5 m long—, and longer ones—up to 6 m long—were taken with pneumatically operated corers (Mackereth, 1958, 1969). Two short cores and nine long cores were collected from Escondido Lake. The long and short cores from Escondido Lake are labelled "les" and "es" respectively. Core lengths are given in Table 1. The location of the coring sites within Escondido Lake are shown in Fig. 1(c).

All cores were cut into 1 m long sections and split open. Upon opening, one half of each core was described, and then subsampled with plastic cubic boxes of 8 cm^3, sealed and weighted for paleomagnetic studies. The number of subsamples taken from each core (N_p) are given in Table 1. Core les10 was lost when it was removed from the corer and core les5 was not studied because it looked completely different from the rest, it seemed to correspond to a sliding.

Subsampling for ^{14}C and $\delta^{13}C$ analyses on pieces of wood, leaves and sediments (N_d in Table 1) and subsampling for palynology analyses were carried out by B. Jackson (Jackson, 1996).

4. Sedimentology

The sediments are granulometrically poorly sorted, clayey-sand and sandy-clay layers are frequently found (Fig. 2). Clay and silt are present in most of the column, some thin layers (5 to 10 cm) associated with coarse and very coarse sand or gravel, allow a correlation between cores taking into account the alternation of colors, the texture and location. Thin well sorted fine and medium sand layers are found (1 to 5 cm), they are characterized by their color and pyroclastic composition. In les8, as an example, 33 tephra layers were determined macroscopically, which were correlated with the sequences of the rest of the cores. The term tephra is assigned to every volcanic product.

The sediments are mainly of pyroclastic origin, the epiclastic material is less abundant. Volcanic glass, ash, tuff and pumice in dark and light color abound. Bad rounded quartz and plagioclase are scarce.

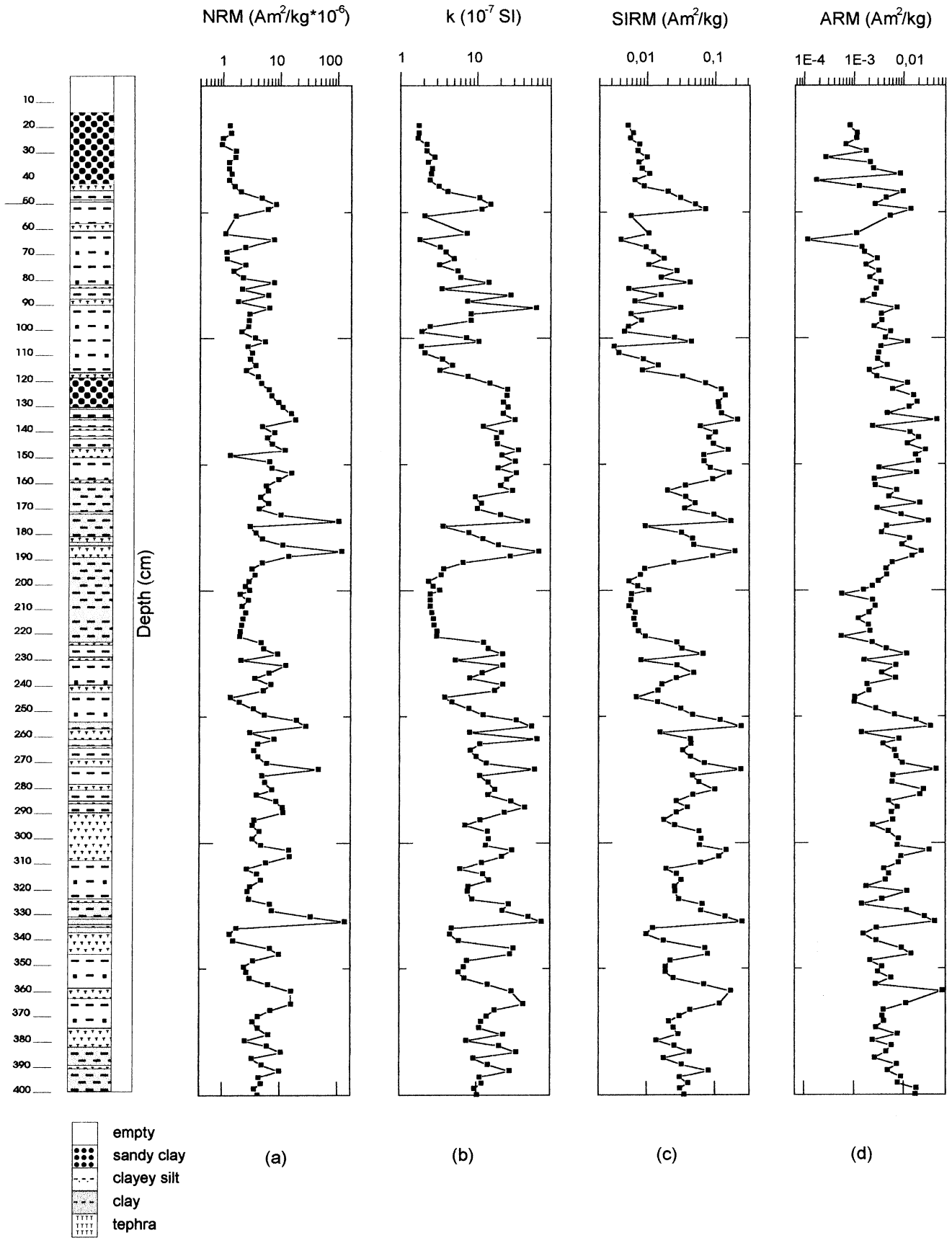

Fig. 2. Sedimentology description and logs of intensity of natural remanent magnetization (a), specific susceptibility (b), saturation isothermal remanent magnetization (c) and anhysteric remanent magnetization (d) for core les8.

Table 2. Radiocarbon dating sample information and calibrated ages.

Tucson lab number	Material	Sent as	Core	Depth (cm)	Date (RCYBP) $\pm\sigma$	Calibrated age $\pm\sigma$
AA-18634	sediment	CO_2	les2	15	840±65	697±65
AA-18636	sediment	CO_2	les2	95	2300±65	2319±65
AA-18630	wood	raw	les2	173	3570±60	3827±60
AA-18629	leaf	raw	les2	265	5235±65	5937±65
AA-18635	sediment	CO_2	les2	330	7950±75	8641±75
AA-18627	sediment	CO_2	les2	375	9565±105	10.536±105
AA-18637	sediment	CO_2	les2	391.5	12.050±95	14.005±95
AA-18628	sediment	CO_2	les2	401.5	12.250±100	14.284±100
AA-18631	clam	raw	es3	0	123.3±0.7%*	
AA-18633	sediment	CO_2	es3	74	1325±55	
AA-18632	wood	raw	les6	233.5–237.5	3640±70	

*:^{14}C activity of 5 years old clam (genus *Diplodon*) was 123%±0.7% of the modern atmospheric activity of ^{14}C.

The most frequent colors in wet sediments are very dark brown (10YR 2/2, the coding used is from the MUNSELL SOIL COLOR CHART) in silty-clay layers; black (10YR 2/1) at the top of many cores, rich in organic matter; very dark grey (10YR 3/1) in sandy-silt layers abundant in volcanic ash, light grey (10YR 7/1) in gravel pumice fragments.

The fine material seen under petrographic microscope shows in some levels abundant biogenic material (diatoms, sponge spicules and pollen in descending order). In some layers diatoms make up about 12% of the sediment. Escondido Lake has abundant wood fragments (Notofagus) and carbon specially between 2 m and 3 m in depth.

The relative amount of volcanic glass varies between 10 and 15% and the relative amount of opaque minerals between 5 and 10%.

5. Radiocarbon Dating

The ages scale for this study is provided by 11 Accelerator Mass Spectrometer (AMS) radiocarbon dates from discrete 1 cm intervals in the cores, obtained by Jackson (1996).

The number of samples taken by Jackson for ^{14}C studies are detailed in Table 1. Eight dates were obtained from les2 and two were obtained from es3. One additional date comes from a wood layer in les6. Pertinent information for each sample, including the dates, in radiocarbon years before present (RCYBP) and calibrated ages, are listed in Table 2.

6. Magnetic Parameters

6.1 Measurements

To procure a magnetic characterization of Escondido Lake sediments, a set of laboratory experiments were carried out on every sample of les8. The following measurements were carried out: intensity of NRM (*Jn*); magnetic susceptibility at low and high frequency (470 and 4700 Hz); isothermal remanent magnetization (IRM) in growing steps until 2T, reaching the saturation isothermal remanent magnetization (SIRM); Back field, in growing steps until cancelling the magnetic remanence; Anhysteric remanent magnetization (ARM), with a direct field of 0.1 mT and an alternate field between 0 and 100 mT, and hysteresis cycles. The associated parameters were computed: F (relative variation of magnetic susceptibility with frequency), S ($\mathrm{IRM}_{-300\,\mathrm{mT}}$/SIRM), coercitive field (B_C), remanent coercitive field (B_{CR}), SIRM/X (X is susceptibility at low frequency); ARM/X; ARM/SIRM.

The utilized equipment is: spinner magnetometer DIGICO, cryogenic magnetometer (2G); susceptibilimeter Bartington MS2, pulse magnetizer developed by Dr. Bohnel and vibrator magnetometer (VSM Molspin).

6.2 Results

The *Jn*, specific susceptibility (k), SIRM and ARM logs show similar characteristics, with correspondence in peaks and troughs (Figs. 2(a), (b), (c) and (d)), although ARM log shows a better affinity with SIRM than with k. The peaks correspond to levels with volcanic ash, and the troughs to levels with organic matter. These results suggest that the behavior of these parameters is determined mainly by the concentration of the magnetic minerals.

Jn changes between 0.06 and 1.4×10^{-4} $\mathrm{Am^2kg^{-1}}$. The lower values of susceptibility are mainly corresponding to lithologies with abundant organic material, and the higher one to tephras.

The specific susceptibility oscillates between 0.02×10^{-6} and 11×10^{-6} $\mathrm{m^3kg^{-1}}$, values corresponding to ferromagnetic materials "sensu latu". F changes between 1 and 3%, this indicates that the contribution of superparamagnetic minerals is negligible (Heller *et al.*, 1991). The higher values of low frequency susceptibility ($0.2 \times 10^{-6} \sim 11 \times 10^{-6}$ $\mathrm{m^3kg^{-1}}$) correspond to tephra layers. These values of susceptibility confirm the macroscopic observations of the tephra layers. The lower values of low frequency susceptibility ($0.025 \times 10^{-6} \sim 0.2 \times 10^{-6}$ $\mathrm{m^3kg^{-1}}$) correspond to material with high proportion of organic matter and fine to very fine

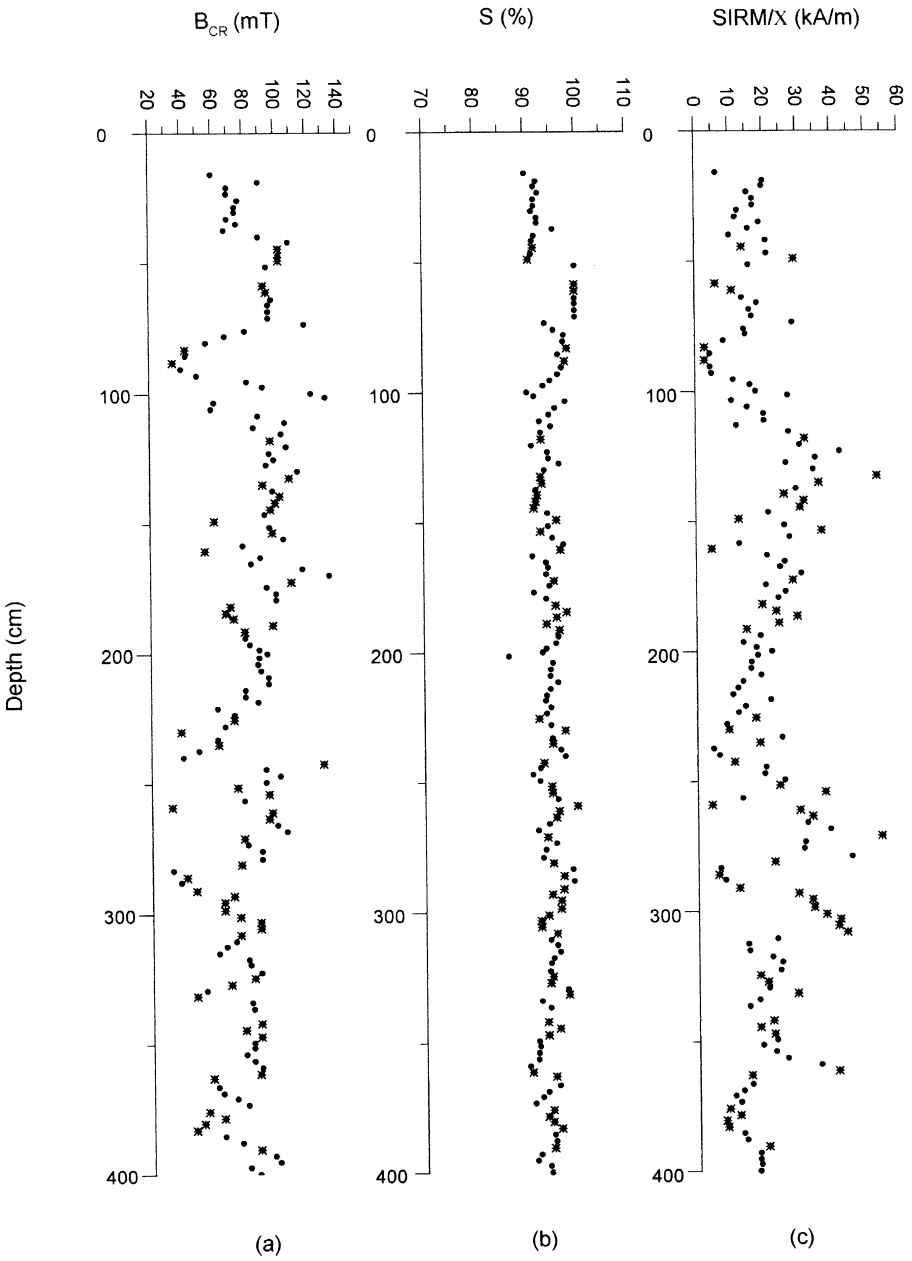

Fig. 3. Logs of Back field (a), *S* parameter (b) and SIRM/*X* ratio (c) for core les8. ∗: samples with abundant tephra, •: the rest of the samples.

grain size.

IRM curves show similar shape for samples with abundant organic matter and samples with high proportion of tephra, along the profile, but they show different parameter values. 80% and 90% of SIRM are obtained with fields of about 150 mT and 300 mT respectively. Every sample of the upper 50 cm of les8 acquires the SIRM with fields of 300 mT, samples from the lower section of the core reach the SIRM with fields between 300 and 950 mT; these values are characteristic of ferrimagnetic materials.

From the Back fields curve the values of B_{CR} are calculated (Fig. 3(a)). B_{CR} values between 30 and 45 mT are mostly found in tephra samples; the carrier could be PSD magnetite and titanomagnetite (Dankers, 1978). B_{CR} values between 45 and 110 mT correspond to samples with a mixed lithology (tephra and organic matter in different rates). These values, not characteristic for pure magnetite, could be caused by the presence of oxidized titanomagnetites, greigite (Roberts and Turner, 1993; Reynolds *et al.*, 1994) and/or antiferromagnetic minerals in low rate, or by the decrease in the size of the grain. B_{CR} values between 110 and 140 mT correspond to samples with abundant organic matter; this environment facilitates the oxidation of titanomagnetites and/or the presence of antiferromagnetic minerals like hematite or goetite (Dekkers, 1988).

Parameter *S* was used to calculate ratio of "soft" minerals to "hard" minerals, Meynadier *et al.* (1992) (Fig. 3(b)). The ratio values vary between 90 and 100%. No evidence of a different behavior for different lithologies is detected. Most of the samples with abundant tephra have ratios close to 100%; one clay sample with very low susceptibility shows the lowest ratio (86%).

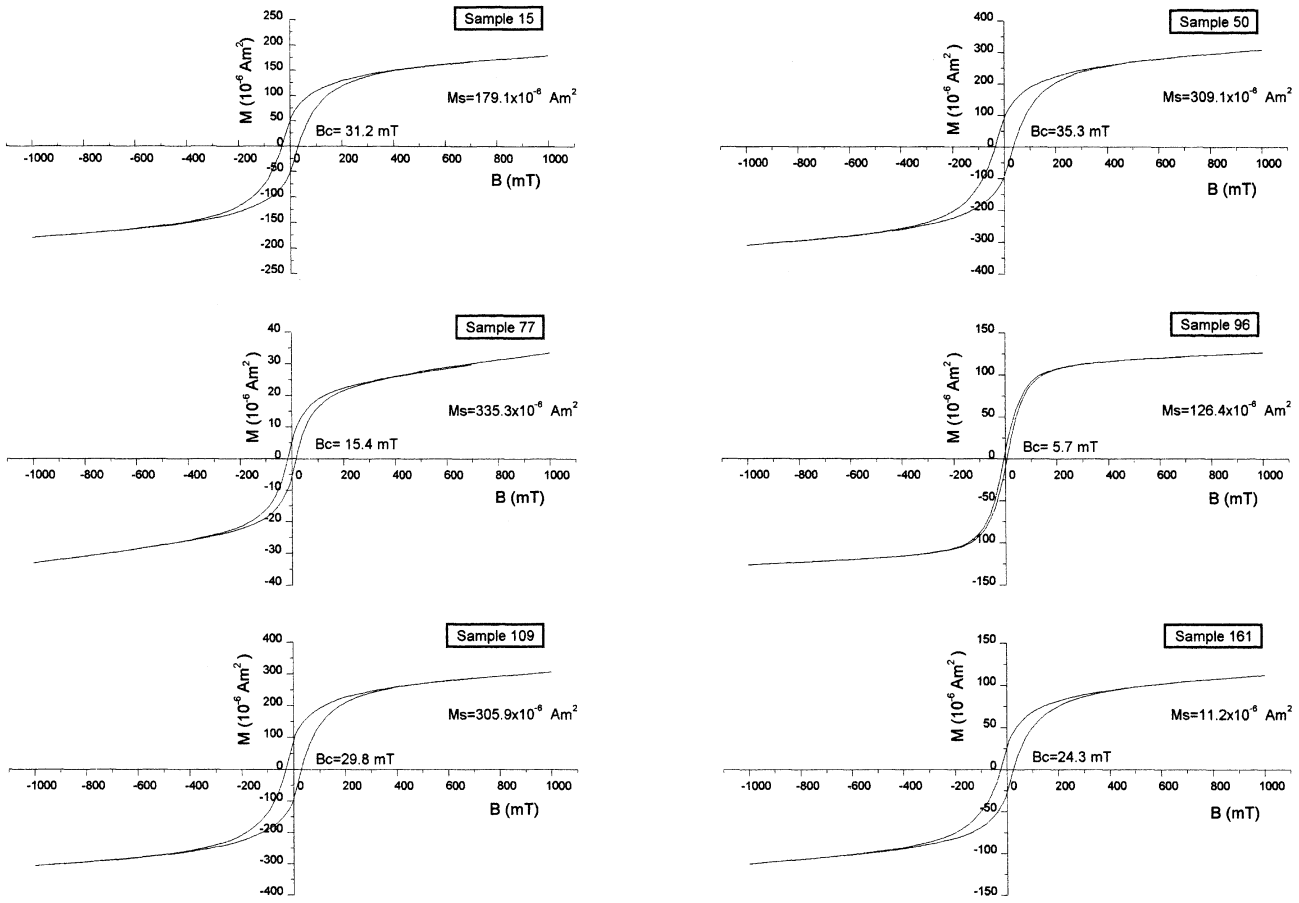

Fig. 4. Hysteresis cycles of several samples. Values of B_C and M_S are indicated.

The SIRM/X ratios are between 4 and 55 KA/m (Fig. 3(c)), which are consistent with pseudosingle domain magnetite (Thompson and Oldfield, 1986).

The relationship between Remanent Saturation Magnetization (M_{RS}) and Saturation Magnetization (M_S) M_{RS}/M_S and B_{CR}/B_C for some analyzed samples was plotted and most of them are in a pseudosingle domain region for magnetite (Day *et al.*, 1977).

Hysteresis cycles of some samples are shown in Fig. 4. Cycles of samples composed almost only by tephra (samples 15, 50 and 109) show very similar shape, but different values of M_S. This result suggests that the concentration is the most changing characteristic and that the carriers are mainly ferrimagnetic minerals with comparatively low coercitive fields. Sample 96 (higher proportion of tephra than of organic matter) shows high M_S and very low B_C (5.7 mT); this is a typical behavior of pseudo single domain or multidomain magnetite. The presence of magnetite in this level is also suggested by the abundance of burnt wood, apparently due to forest fires. Sample 161 (higher proportion of fine sediments than of tephra) shows a similar hysteresis loop to samples with abundant organic matter and tephra and a B_C about 24.3 mT. Sample 77 (pure sediment) shows, as expected very low M_S.

The different lithologies show paramagnetic contribution to the M_S. This contribution is between 23 and 24% in tephra samples, and between 16 and 35% in samples with a high proportion of organic matter.

7. Paleomagnetic Studies

7.1 Measurements

The *Jn* and directions (Declination, D and Inclination, I) of NRM were measured using a Digico, a Molspin and a 2-G cryogenic magnetometer. Magnetic susceptibility measurements were made using a Bartington susceptibilimeter and k was calculated.

Stability of the NRM was investigated by alternating-field (AF) demagnetization. For one core, one sample of each four was chosen as pilot sample. They were demagnetized successively at 5, 10, 15, 20, 30 and 35 mT peak field (Fig. 5). Most of the samples showed no systematic change in the direction of their remanent magnetization during AF demagnetization; few of them showed a viscous magnetization, probably picked up in laboratory fields, which could easily be removed by AF demagnetization at 5 or 10 mT. Median destructive fields are in the range 10–35 mT, similar to those generally found for other Holocene lake sediments. This result favours the assumption that magnetically soft carriers are present in the samples. Taking into account these results, every sample was demagnetized at 10 mT peak field.

7.2 Results

Jn, k, D and I of stable remanence logs were made. Since

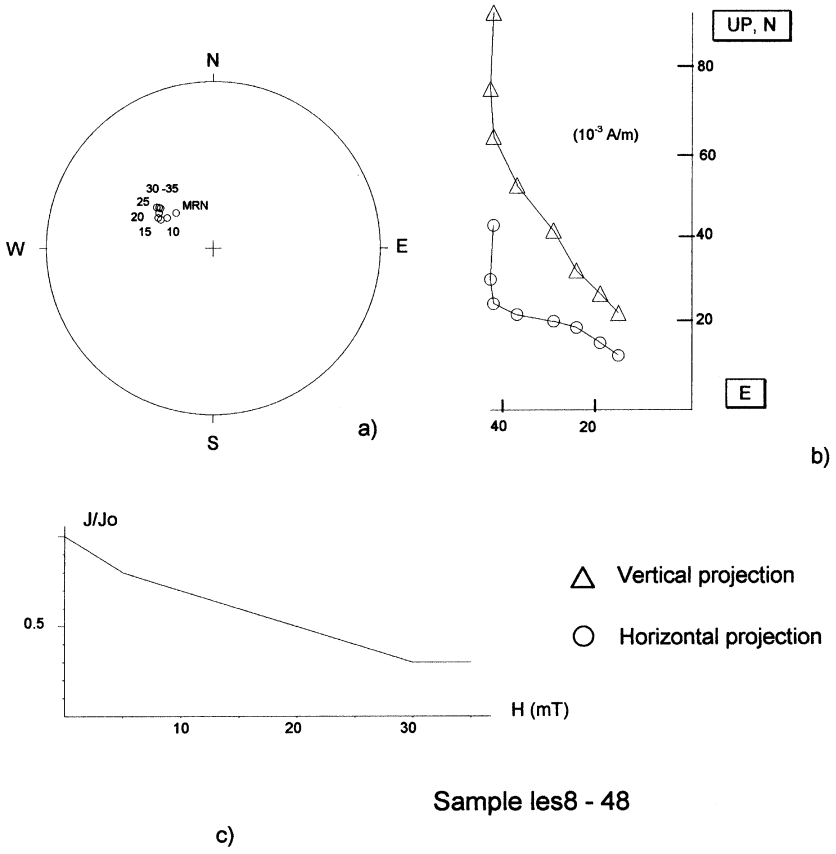

Fig. 5. Stereographic projections of remanence directions, relative intensity plots, and Zijderveld diagrams for progressive AF demagnetization of sample les8-48.

the cores were not orientated relative to the magnetic north, the *D* values for each core are centred about the average declination. As mentioned above, the *Jn* and *k* logs from each core show the same trend; therefore both, *Jn* and *k* logs can be used to define tie-lines to describe the lithostratigraphic correlation of cores of the same lake. These tie-lines were consistent with the lithology. Figure 6 shows the *k* logs corresponding to every core from Escondido Lake and the correlation tie-lines. This correlation confirms the relationship suggested by visual inspection of distinctive layers of the sediment of both cores.

Jn and *k* logs allowed also the correlation between es3 and les2; this correlation shows that approximately 23 cm of sediment was lost from les2. Core les2 was chosen as "master" core. The depth scales of all the cores were adjusted to the depth scale of the master core using lithology, *Jn* and *k* tie-lines for correlation. Figure 7 shows the alignment of the major peaks and troughs along the *Jn* logs, after the stretching process to the common depth scale.

D and *I* logs may be used to infer chronostratigraphic within lake correlation and between lake correlation of the sedimentary sequences, but this is not easy because noises of different origins can affect these values.

One of the most important problems to take into account is the presence of abundant tephra layers along the sequence. The tephra layers were identified from the lithologic profiles and also from the *k* logs, because, as it was mentioned, these layers have higher values of susceptibility. The tephra layers have a different chronological meaning, because they were deposited instantaneously. For this reason, to carry out a chronological correlation these layers can not be considered comparable to the rest of the sediments. On the other hand, in general, the *D* and *I* values corresponding to the tephra layers of these sediments are very different from the mean values of these parameters and they are not consistent among cores. This event shows that in this case, tephra are not very good magnetic recorder of directions. This conclusion is consistent with the fact that generally, the tephra layers are coarser. This behavior of volcanic ashes was also reported by Peng and King (1992). After the identification of the tephra layers, they were removed from the sequence and the gaps that were produced along the profiles by the removal were closed, obtaining a *shortened depth*, (Figs. 8 and 9). Figure 8 shows the calibrated ages along the sequence. The upper section of the sequence (younger than 10536 years) shows a deposition rate approximately constant, and a jump between 10536 and 14005 years is evident, which could be explained by a hiatus.

8. Stacking and Transformation into a Time-Scale

A stacking process, consisting in arithmetical average, with previous interpolation every 2 cm, was carried out until a depth of 230 cm, because for higher depths there are records of only one core. In order to obtain the *I* stacked curve, all

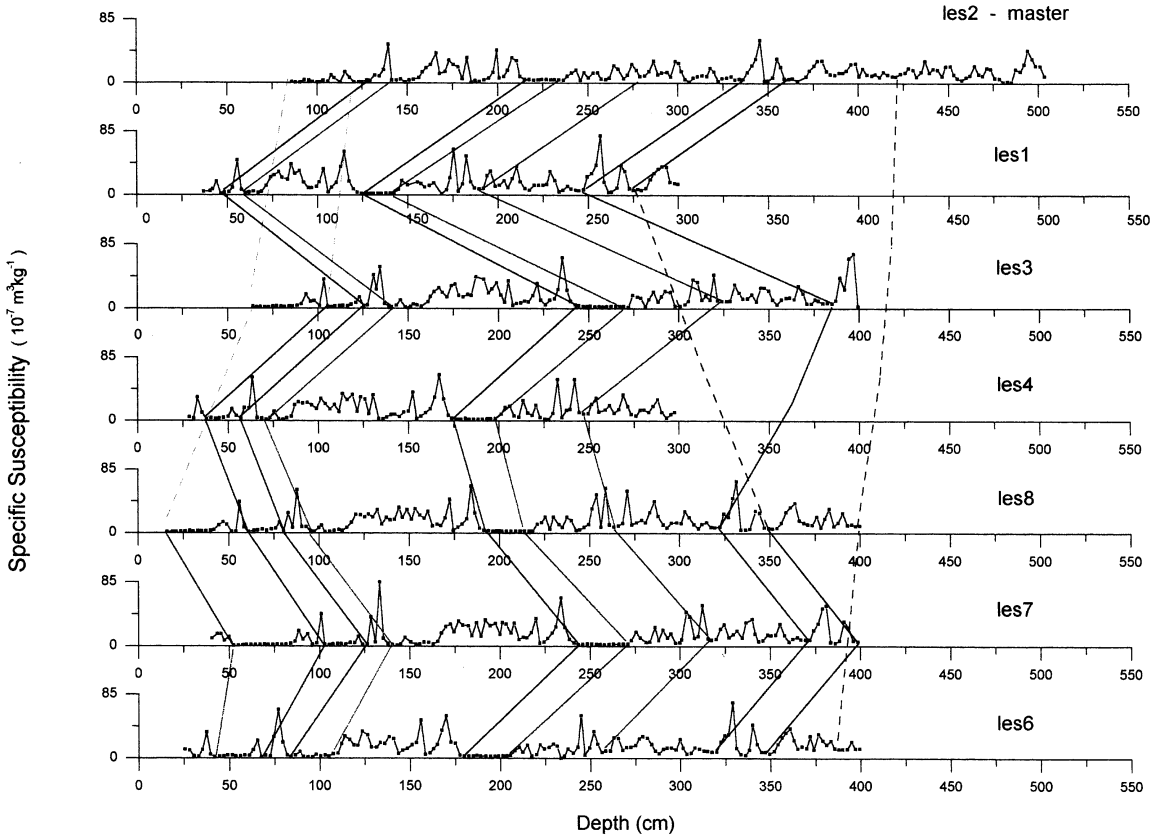

Fig. 6. *k* logs corresponding to every core from Escondido Lake and the correlation tie-lines.

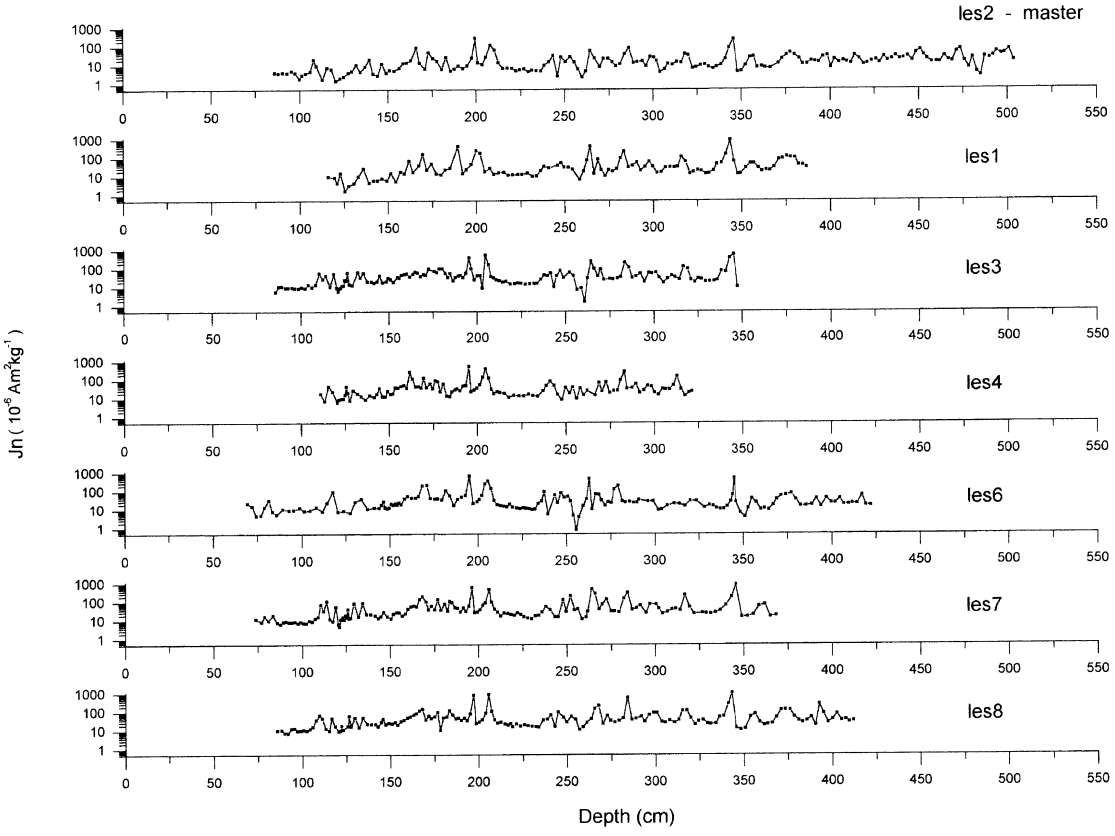

Fig. 7. *Jn* logs for Escondido Lake after adjusting to the depth scale of les2 (master core), using *Jn* and *k* tie-lines for correlation.

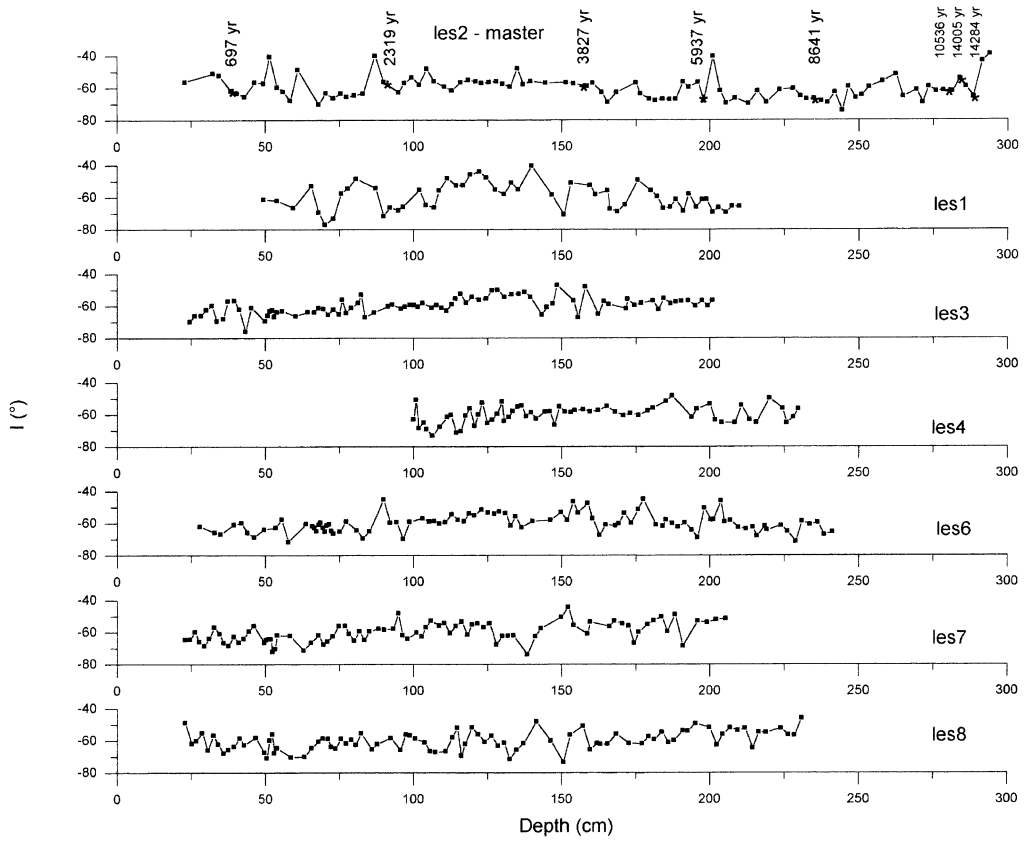

Fig. 8. Inclination logs vs. *shortened depth*, after the tephra levels were removed. The zero of the depth scale corresponds to the top of the sediment. The calibrated ages are indicated.

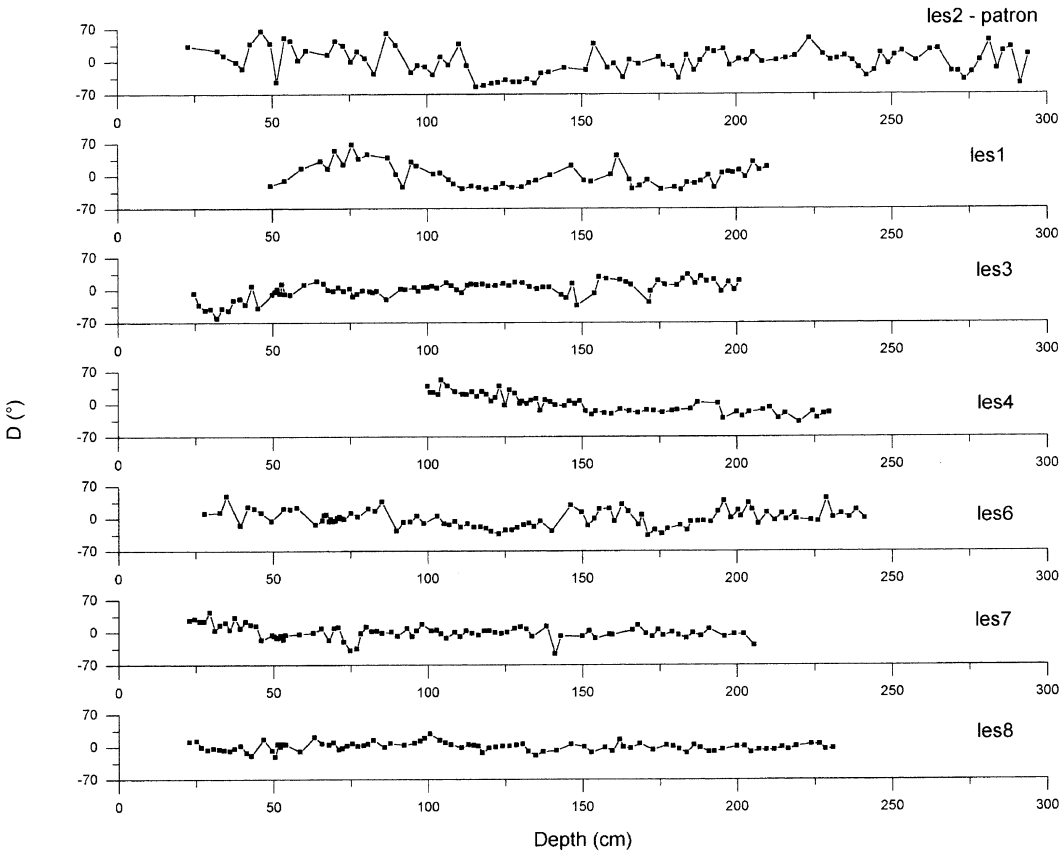

Fig. 9. Declination logs vs. *shortened depth*, after the tephra levels were removed. The zero of the depth scale corresponds to the top of the sediment.

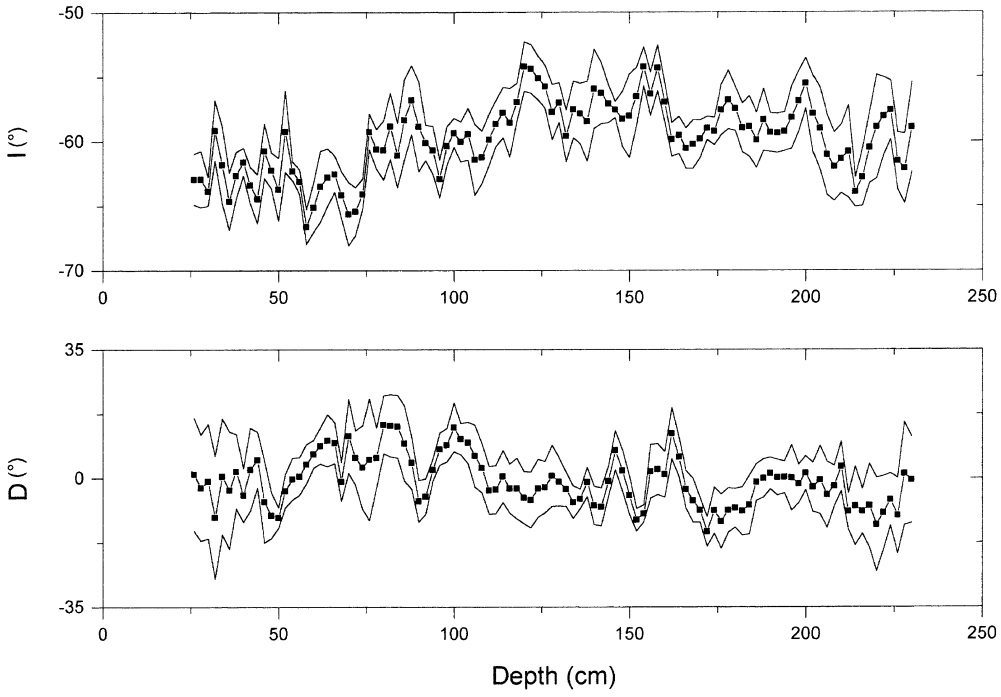

Fig. 10. Stacked Declination and Inclination logs vs. *shortened depth*. The standard deviation is shown.

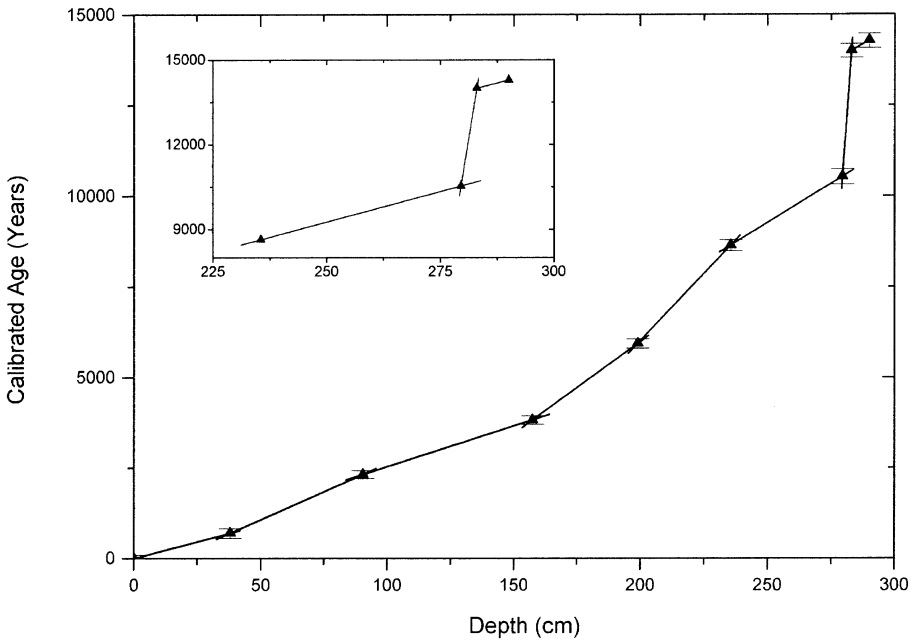

Fig. 11. Calibrated ages vs. *shortened depth* at Escondido Lake and a linear interpolation between points.

cores were used, but for *D* stacked curve the core les2 was removed, because it shows higher amplitude of oscillation than the other cores. Figure 10 shows *D* and *I* vs. *shortened depth*. The error interval, considering the standard deviation is shown. The choice of arithmetical average instead Fisher statistics is discussed below.

Figure 11 shows the calibrated ages vs. *shortened depth* for the first 250 cm. A fitting was made, joining each pair of dating (linear interpolation) with segments. When the two higher radiocarbon dating are taken into account, there is a sudden change of slope and, finally, the last segment has a similar slope than those of the first segments. This behavior may be explained, as mentioned above, by a hiatus, and then a sedimentation rate for the lower section, not very different from the rate of the rest of the section.

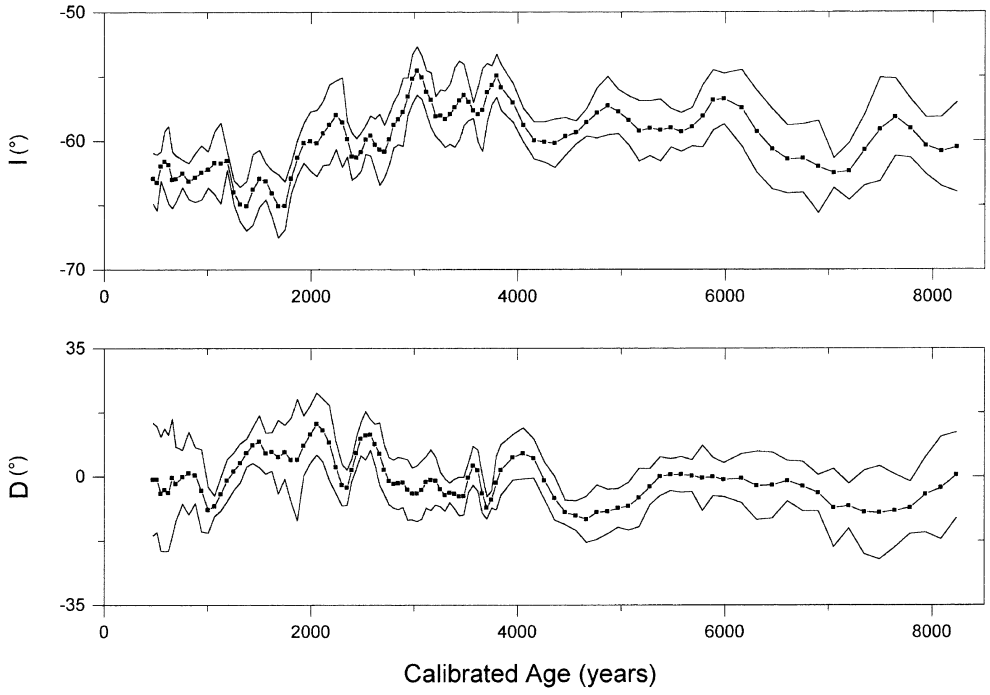

Fig. 12. *D* and *I* logs as function of calibrated ages. The depth was transformed to calibrated ages, using the linear interpolation between datings. The standard deviation is shown.

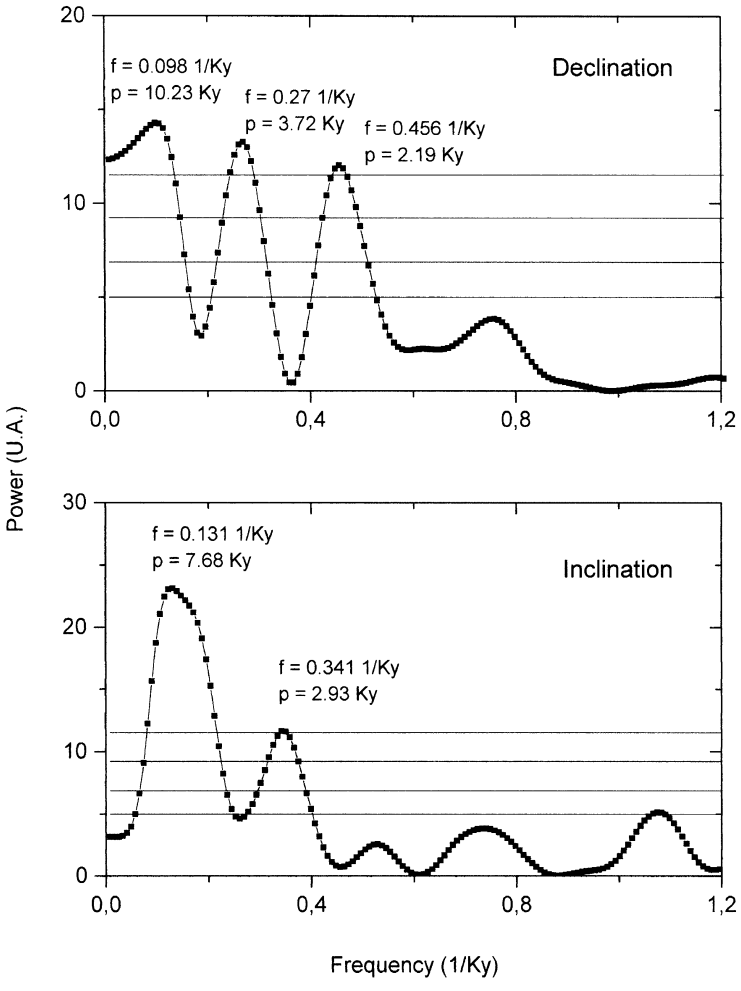

Fig. 13. Spectral analysis of *I* and *D* data by Lomb-Scargle method.

Table 3. Periods identified by Lomb-Scargle method and Bretthorst code for Inclination and Declination.

	Periods for Inclination (years)		Periods for Declination (years)		
Lomb-Scargle	7680	2930	10230	3720	2050
Bretthorst	7758	2637	10598	3993	2045

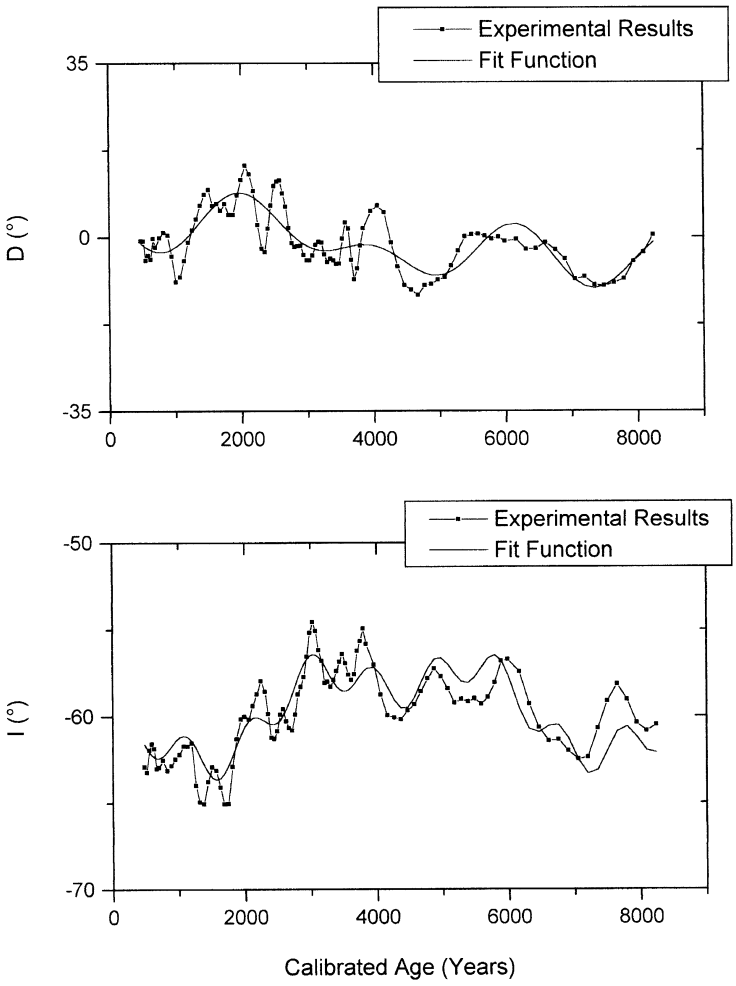

Fig. 14. Fit functions for I and D obtained by Bretthorst code, compared with the experimental results.

9. Spectral Analyses

D and I logs vs. calibrated age were built for the section of the sequence younger than the hiatus. A smoothing (running average of three points) was applied to the values of D and I (Fig. 12) and the error interval is shown. The frequencies present in the records were identified by a spectral analysis made with Lomb-Scargle method (Scargle, 1982; Horne and Baliunas, 1986) (Fig. 13). Two frequencies were resolved in I, one with significance level higher than 0.1% (f_a = 0.131 Ky^{-1}) and a second one with significance level of just 0.1% (f_b = 0.341 Ky^{-1}); they correspond to periods of 7680 and 2930 years, respectively. Two frequencies were also identified for D data, both with significance level higher than 0.1% (f'_a = 0.27 Ky^{-1}, f'_b = 0.456 Ky^{-1}), they correspond to periods of 3720 and 2190 years, respectively. A third frequency is identified (0.098 Ky^{-1}), but it is to consider that it corresponds to a period of 10230 years, longer than the time span of the record. The results are summarized in Table 3.

To make sure that the identified frequencies are not artifacts, the spectral analysis was carried out using a square function of about 5000 years, as window for the Inclination data, and running this window from lower to higher ages; six intervals were analysed. Two frequencies are obtained from the different set of data, one about 0.36 Ky^{-1}, and a second one about 0.16 Ky^{-1}; the higher frequency is comparable to f_b and the lower one may correspond to f_a. The lack of a better coincidence with f_a may be caused by the limited time span of the window. The same procedure was used for D data. In this case the identification of common frequencies is more difficult. For different intervals, frequencies between

0.42 and 0.59 Ky^{-1} are found, which may correspond to f'_b; a second frequency of about 0.2 Ky^{-1}, which may correspond to f'_a is identified, but only for three intervals.

To fit the data with a function containing different frequencies a code from Bretthorst (Bretthorst, 1988, 1990a,b,c) was used. The procedure is the following: the experimental data and one of the estimated frequencies (by Lomb-Scargle method) are given and a first fit function is obtained with a frequency, which is fitted from the estimated value given as input. The residual between the experimental data and this first function is calculated. An spectral analysis is applied to this residual to confirm the disappearance of the given frequency and to find a new one. Both frequencies are then used as input to construct the new fit function. This process is repeated inasmuch as necessary with the data of the residual and the different frequencies (one at a time) are estimated.

The frequencies obtained from the application of this subroutine to the I and D data are summarized in Table 3 and the fit functions are shown in Fig. 14.

10. Discussion

Although the main carriers are ferrimagnetic minerals (pseudo single domain magnetite was detected) the presence of greigite is suggested by the stability of the remanence, the relative high values of median destructive field and the high values of SIRM/X (Hallam and Maher, 1993 and Roberts, 1995). If this assumption is accepted, it is notorious that the greigite would be a diagenetic *euxinic* material present in layers with abundant volcanic ash, as well as, in layers with high proportion of organic matter. The presence of a low proportion of antiferromagnetic material is suggested by high values of B_{CR} (Dekkers, 1988). The origin of this fraction may be either primary (magmatic) or secondary (detritic by erosion of the surrenders or diagenetic).

On account of the evidence of a lot of magmatic events, it is not easy to carry out paleoenvironmental relations. The susceptibility increases smoothly with growing depth; this result suggests a decrease of organic matter with depth and it is consistent with the paleoclimatic conclusions obtained with the palynological results (Jackson, 1996).

As mentioned before the transformation into a time scale was carried out by a linear fitting between each pair of dating. Also a good fitting was obtained with a second order polynomial, when the two higher ages are not taken into account. This polynomial could be explained by a hypothesis of compacting along the section, with deposition rates from about 1 mm/year in the upper part until about 0.15 mm/year in the lower part. If the two higher radiocarbon dating are included, this fitting becomes inadequate. This behavior may be explained, as mentioned above, by a hiatus, and then a sedimentation rate for the lower section, not very different from the rate of the rest of the section. The results obtained with this fitting does not differ from those obtained with the linear interpolation.

The possibility of a hiatus that explains the bad adjustment of the higher ages with both fittings is supported by the suggestion of the palynological study. Jackson (1996) delineated nine zones, from the pollen record. These zones suggest dominant arboreal taxa by 13300 RCYBP, but with indicators of an open forest, and a relatively dry climate. This lasted until 12800 RCYBP, when a more dense closed *Nothofagus* forest developed, and moister levels increase from the previous zone. This assemblage gave way to less dense forest assemblage at approximately 11200 RCYBP. Long-distance-transport elements and herbaceous taxa increased, and a drier climate is inferred. Jackson (1996) suggests that the drier conditions are similar to conditions inferred for the late glacial period, and lasted until about 8900 RCYBP and that this assemblage would represent the younger Dryas cooling event seen in the Antarctic ice cores.

When the profiles of I and D of every core were observed, the I logs seem more consistent than D logs. The amplitude of oscillation of D are dissimilar for different cores, for this reason les2 was removed in the stacking procedure for D. It seems evident that D data are less reliable than I data. To confirm this appreciation, Fisher statistic was applied in two ways: i) using the experimental Inclination values and assuming the geocentric dipole field value for Declination ($D = 0^\circ$), and ii) using the experimental Declination values and assuming the geocentric dipole field value for Inclination ($I = -60^\circ$). the parameter α_{95} was better for the first test ($\alpha_{95} = 4.2^\circ$) than for the second one ($\alpha_{95} = 7.7^\circ$). For this reason, a stacking procedure consisting in arithmetical average of Declination and Inclination was used. This method allows an unconstrained handling of Declination and Inclination.

The interpolation used before stacking had the only aim of obtaining data at the same horizons for each core, but it did not produce "new data"; in fact the total number of data is very similar to the experimental values. For this reason the final curves are reliable and can not be considered an artifact.

The results of Escondido Lake were compared with the paleomagnetic results reported by Creer *et al.* (1983) for lakes of the same area. The comparison is qualitative, because Creer *et al.* used radiocarbon ages. The Inclination and Declination logs show correspondence, although the distinctive features of the logs appear in older ages in Escondido logs, due to the employment of calibrated ages. The correspondence is better for Inclination than for Declination. For Declination two peaks, at about 1500 and 2000 years, are present in both records, but the relative amplitudes are different, for Escondido Lake the higher peak corresponds to 2000 years and for the results presented by Creer *et al.* (1983), the higher peak appears at about 1500 years.

The spectral analysis was carried out with smoothed data. The running average of three points means a range of about 150 years, then very high frequencies are not identified. But these frequencies are much higher than those extracted from spectral analyses. The results obtained by the two methods (Lomb-Scargle and Bretthorst) are consistent, and the fit functions constructed have a good agreement with the experimental data. The lower frequency identified by spectral analyses for D corresponds to a period longer than the time span of the record, then it is less reliable than the other frequencies; it could be consider a long wavelength trend.

Another confirmation than D data are less reliable than I data was obtained by the spectral analysis through windows. As mentioned before, the frequencies obtained for I with this procedure are consistent, while those found for D show some differences for different intervals.

Hagee and Olson (1989) used data from one core of another lake of the same area and obtained a period of 8000 years for declination and inclination. Peng and King (1992) found a similar period in inclination and declination records from lake sediments of Hawaii. They also identified periods of about 3500 years, which could be comparable with the period found in this paper. Periods of about 1000 years and between 2000 and 3500 years were also found by several authors for North America, Europe and Australia (Hagee and Olson, 1989; Creer and Tucholka, 1982, 1983; Kane, 1989). It is to mention than although only Creer and Tucholka (1982) use calibrated ages, the comparisons can be made because the aim is to identify similar ranges of periods.

The longer period may be related to dipolar variations, while the shorter periods may be associated to non dipolar variations. This suggestion could explain why the shorter periods show different values in each area.

It is important to mention that the identified periods are only established for the particular time span of the record and there is no reason to suppose that they are stationary.

11. Conclusions

The main carrier are ferrimagnetic minerals as pseudo single domain magnetite. A low proportion of antiferromagnetic material of primary or secondary origin is also suggested.

The transfer function depth-age suggests the existence of a hiatus supported by the suggestion of the palynological study (Jackson, 1996).

Inclination data show two very well defined periods: a long period (about 7700 years) and a short one (between 2900 and 2600 years according to the method).

Declination data, although less reliable, show two intermediate periods of about 3700 and 2200 years, and a long wavelength trend.

Periods within the same intervals are found by another authors for lakes from the same area, North America, Europe and Australia.

Acknowledgments. The authors wish to thank Antorchas Foundation, which supported the field work and the transportation of the Mackereth corer from Argentina back to United Kingdom. They also thank Universidad de Buenos Aires, Universidad Nacional del Centro de la Provincia de Buenos Aires, CONICET and University of Wisconsin for their support.

They would like to take this opportunity to express their gratitude to PROGEBA Institute for kindly making the place available to carry out the sampling, and also for the logistic help.

They are greatly indebted to Dr. Bretthorst for his generous help in interpreting his code and for the fruitful discussions, and to Dr. Lund and an anonymous reviewer for their worthy suggestions.

The Mackereth corer and the collaboration of Mr. Alan Pike were kindly provided by the University of Edinburgh.

References

Bretthorst, G. L., Bayesian spectrum analysis and parameter estimation, in *Lecture Notes in Statistics*, edited by J. Berger, S. Fienberg, J. Gani, K. Krickeberg, and B. Singer, vol. 48, Springer-Verlag, New York, 1988.

Bretthorst, G. L., Bayesian analysis. I. Parameter estimation using quadrature NMR models, *J. Magn. Reson.*, **88**, 533–551, 1990a.

Bretthorst, G. L., Bayesian analysis. II. Model selection, *J. Magn. Reson.*, **88**, 552–570, 1990b.

Bretthorst, G. L., Bayesian analysis. III. Applications to NMR signal detection, model selection and parameter estimation, *J. Magn. Reson.*, **88**, 571–595, 1990c.

Creer, K. M. and P. Tucholka, The shape of the geomagnetic field through the last 8,500 years over part of the Northern Hemisphere, *J. Geophys.*, **51**, 188–198, 1982.

Creer, K. M. and P. Tucholka, On the current state of lake sediment paleomagnetic research, *Geophys. J. of the R.A.S.*, **74**, 1, 223–238, 1983.

Creer, K. M., D. A. Valencio, A. M. Sinito, P. Tucholka, and J. F. Vilas, Geomagnetic secular variations 0–14000 yr BP as recorded by lake sediments from Argentina, *Geophys. J. Roy. astr. Soc.*, **74**, 1, 109–222, 1983.

Dankers, P. H. M., Magnetic properties of dispersed natural iron-oxides of known grain-size, Ph.D. Thesis, Rijksuniversiteit te Utrecht, 143 pp., 1978.

Day, R., M. Fuller, and V. A. Schmidt, Hysteresis properties of titanomagnetites: Grain size and compositional dependence, *Phys. Earth Planet. Int.*, **13**, 260–267, 1977.

Dekkers, M. J., Some rock magnetic parameters for natural goethite, pyrrhotite and fine-grained hematite, Ph.D. Thesis, State University Utrecht, 231 pp., 1988.

Feruglio, E., Nota preliminar sobre la hoja 40b, San Carlos de Bariloche, *Boletín Informaciones Petroleras*, **18**, 200, 26–64, 1941.

Gogorza, C. S., I. Di Tommaso, A. M. Sinito, B. Jackson, H. Nuñez, K. M. Creer, and J. F. Vilas, Preliminary results from paleomagnetic records on lake sediments from South America, *Studia of Geophys. et Geodet.*, **42**, 12–29, 1998.

González-Bonorino, F., Geología del área entre San Carlos de Bariloche y Llao-Llao, Departamento Recursos Naturales y Energía, Fundación Bariloche, Public., 16, 1973.

González-Bonorino, F., Esquema de la evolución geológica de la Cordillera Nordpatagónica, *Asoc. Geol. Arg. Rev.*, **34**, 3, 184–202, 1979.

González-Díaz, E. and F. Nullo, Cordillera Neuquina, in *Geología Regional Argentina*, Academia Nacional de Ciencias de Córdoba, II, pp. 1099–1147, 1980.

Hagee, V. L. and P. Olson, An analysis of paleomagnetic secular variation in the Holocene, *Phys. Earth Planet. Int.*, **56**, 266–284, 1989.

Hallam, D. F. and B. A. Maher, A record of reversed polarity carried by the iron sulphide greigite in British early Pleistocene sediments, *Earth Planet. Sci. Lett.*, **121**, 71–80, 1993.

Heller, F., X. M. Liu, T. S. Liu, and T. C. Xu, Magnetic susceptibility of loess in China, *Earth Planet. Sci. Lett.*, **103**, 301–310, 1991.

Horne, J. H. and S. L. Baliunas, A prescription for period analysis of unevenly sampled time series, *Astrophys. J.*, **302**, 757–763, 1986.

Jackson, B. M., Paleoenvironmental Record from Lago Escondido, Rio Negro Province, Argentina, Thesis, University of Wisconsin, 136pp., 1996.

Kane, R. P., Periodicities in the Time-Series of geomagnetic inclination during the last 9000 years, recorded in sediment cores from Lake Kasumigaura, Japan, *J. Geomag. Geoelectr.*, **41**, 525–532, 1989.

Mackereth, F. J. H., A portable core sampler for lake deposits, *Limnol. Oceanogr.*, **3**, 181–191, 1958.

Mackereth, F. J. H., A short core sampler for sub-aqueous deposits, *Limnol. Oceanogr.*, **14**, 145–151, 1969.

Meynadier, L., J. P. Valet, R. Weeks, N. J. Shackleton, and V. L. Hagee, Relative geomagnetic intensity of the field during the last 140 ka, *Earth Planet. Sci. Lett.*, **114**, 39–57, 1992.

Peng, L. and J. W. King, A late Quaternary geomagnetic secular variation record from Lake Waiau, Hawaii, and the Question of the Pacific nondipole low, *J. Geophys. Res.*, **97**, B4, 4407–4424, 1992.

Reynolds, R. L., M. L. Tuttle, C. A. Rice, N. S. Fishman, J. A. Karachewski, and D. M. Sherman, Magnetization and geochemistry of greigite-bearing Cretaceous strata, North Slope Basin, Alaska, *Am. J. Sci.*, **294**, 485–528, 1994.

Roberts, A. P., Magnetic properties of sedimentary greigite (Fe_3S_4), *Earth Planet. Sci. Lett.*, **134**, 227–236, 1995.

Roberts, A. P. and G. M. Turner, Diagenetic formation of ferrimagnetic iron sulphide minerals in rapidly deposited marine sediments, New Zealand, *Earth Planet. Sci. Lett.*, **115**, 257–273, 1993.

Scargle, J. D., Studies in astronomical time series analysis. II. Statistical aspects of spectral analysis of unevenly spaced data, *Astrophys. J.*, **263**, 835–853, 1982.

Thompson, R. and F. Oldfield, *Environmental Magnetism*, 225pp., Allen & Unwin Ltd., 1986.

C. S. G. Gogorza (e-mail: cgogorza@ifas.exa.unicen.edu.ar), A. M. Sinito, I. Di Tommaso, J. F. Vilas, K. M. Creer, and H. Nuñez